s	standard deviation
T	thermodynamic temperature, K
V^E	excess volume, $cm^3\ mol^{-1}$
x	mole fraction
M	morpholine
DMF	*N,N*-dimethylformamide
DMSO	dimethyl sulfoxide

Registry No. DMF, 68-12-2; morpholine, 110-91-8; methanol, 67-56-1; acetone, 67-64-1; benzene, 71-43-2; chloroform, 67-66-3; dimethyl sulfoxide, 67-68-5.

Literature Cited

(1) Awwad, A. M.; Allos, E. I. *J. Pet. Res. (Iraq)* **1986**, *5*, 95.
(2) Awwad, A. M.; Al-Madafi, S. F.; Jbara, K. A. *J. Chem. Thermodyn.* **1985**, *17*, 105.
(3) Al-Mashhadani, A. M.; Awwad. A. M. *Thermochim. Acta* **1985**, *89*, 75.
(4) Riddick, J. A.; Bunger, W. B. *Organic Solvents*; Wiley-Interscience: New York, 1970; Vol. II.

Received for review April 21, 1987. Accepted December 23, 1987.

Gas Viscosities of Azeotropic Mixtures of the Halogenated Hydrocarbons R500, R502, and R503

Mitsuo Takahashi, Chiaki Yokoyama, and Shinji Takahashi*

Chemical Research Institute of Non-Aqueous Solutions, Tohoku University, Sendai 980, Japan

Gas viscosities of azeotropic mixtures R500 (dichlorodifluoromethane (R12)–1,1-difluoroethane (R152a)), R502 (chlorodifluoromethane (R22)–chloropentafluoroethane (R115)), and R503 (chlorotrifluoromethane (R13)–trifluoromethane (R23)) were measured with an oscillating disk viscometer of the Maxwell type at 273.15–423.15 K up to 7.5 MPa. Two empirical equations for the viscosities were obtained; one is for the atmospheric viscosities as a function of temperature, and the other is for the viscosities in the whole range of the present measurement as a function of temperature and density.

The measurements of gas viscosities of halogenated hydrocarbons under pressure are being continued by the present authors, and the viscosity data for dichloromethane (R12), chlorotrifluoromethane (R13), bromotrifluoromethane (R13B1), chlorodifluoromethane (R22), 1,2,2-trichloro-1,1,2-trifluoroethane (R113), 1,2-dichloro-1,1,2,2-tetrafluoroethane (R114), chloropentafluoroethane (R115), 1-chloro-1,1-difluoroethane (R142b), and 1,1-difluoroethane (R152a) were reported previously (*1–5*). Gas viscosities of azeotropic mixtures of halogenated hydrocarbons R500, R502, and R503 are described in the present paper.

Table I shows the composition and the physical properties of azeotropic mixtures (*6*), and Table II shows the physical properties of the components of azeotropic mixtures (*6*).

The gas viscosity of R500 was measured by Latto et al. (*7*) in the temperature range from 244 to 360 K at atmospheric pressure but has not been measured under pressure. The gas viscosities of R502 and R503 have not been measured in any pressure range.

The atmospheric viscosity vs temperature equations were obtained for R500 (*7*, *8*) on the basis of the experimental viscosity values (*7*), and the equation of the same type was obtained for R502 (*8*) on the basis of predicted values (*9*). Description for the viscosity of R503 was not found in the literature.

Experimental Section

***Viscosity Measurement* (*10*, *11*).** The viscosity was measured with an oscillating disk viscometer of the Maxwell type shown in Figure 1. The main part is the suspension system shown in Figure 2, which is composed of an oscillating stainless steel disk (A), a fine suspension quartz wire (C), two fixed stainless steel disks (K), and a stainless steel stem (B) with a nickel-plated glass mirror and with a Permalloy piece (F). In this system the distance between the oscillating disk and the upper fixed disk should be equal to the distance between the oscillating disk and the lower fixed disk at any ambient temperatures. In order to satisfy this requirement, three quartz tubes (M) were inserted between the upper fixed disk and a fixing disk (I), and three stainless steel spacers (L) were inserted between the two fixed disks, and the length of the stem was adjusted. The three quartz tubes and the three spacers were fixed by using three stainless steel rods (N), nuts (O, Q), and springs (P). The characteristics of the suspension system are shown in Table III.

Newell's theory (*12*) was used for analysis in a manner similar to that used by Iwasaki and Kestin (*13*). The apparatus constant, C_N, was determined experimentally with nitrogen as standard at 298.15, 323.15, 348.15, 373.15, and 398.15 K in the pressure range from 0.1 to 6 MPa. The viscosity values of nitrogen recommended by Hanley et al. (*14*, *15*) were used and the density of nitrogen was calculated from a BWR equation of state (*15*). The obtained C_N values were nearly constant, independent of temperature and pressure. The mean value was 1.1338 and the probable error was 0.03% for 39 experimental points. The error in the viscosity determination was estimated to be less than 0.3% considering the error of logarithmic decrement (0.25%) and the error of the period of oscillation (0.01%).

***Density Measurement* (*16*).** In this study the density was measured at the temperature and pressures at which the viscosity was measured. A schematic diagram of the apparatus is shown in Figure 3. A high-pressure pipet (B), the detail of which is shown in Figure 4, was designed for the measurement in the critical region and was located at the same level as the oscillating disk. Sample gas was introduced into the high-pressure pipet at the same temperature and pressure at which the viscosity was measured, and then introduced into an expansion system composed of a mercury manometer (H), a connecting capillary (D), and four glass cylinders (K). The expansion system was thermostated at 298.15 K, and evacuated before introducing the gas. Residual gas in the pipet was

0021-9568/88/1733-0267$01.50/0

Table I. Physical Properties of Azeotropic Mixtures

	composition	mol wt[a]	T_b,[a] K	T_c,[a] K	P_c,[a] MPa	ρ_c,[a] kg·m^{-3}
R500	R12 (73.8 wt %) + R152a (26.2 wt %)	99.31	239.7	378.7	4.43	497
R502	R22 (48.8 wt %) + R115 (51.2 wt %)	111.6	227.6	363	4.27	559
R503	R13 (59.9 wt %) + R23 (40.1 wt %)	87.5	184.5	292.7	4.19	491

[a] Mol wt, molecular weight; T_b, boiling point at atmospheric pressure; T_c, critical temperature; P_c, critical pressure; ρ_c, critical density. Reference *6*.

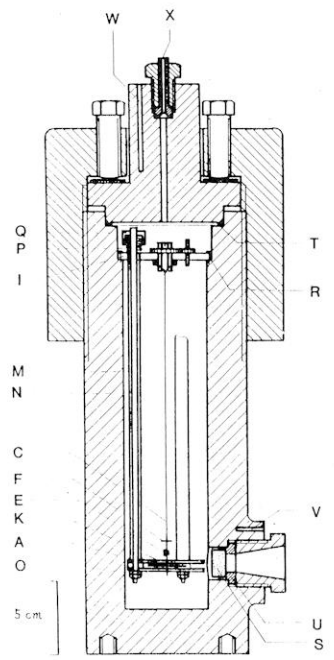

Figure 1. Viscometer: A, oscillating disk; B, stem; C, suspension wire; D, bolt; E, mirror; F, Permalloy piece; G, gear; H, nut; I, fixing disk; J, gear; K, fixed disk; L, spacer; M, quartz tube; N, rod; O, nut; P, spring; Q, nut; R, bolt; S, window; T, packing; U, ring; V and W, well for thermocouple; X, gas inlet.

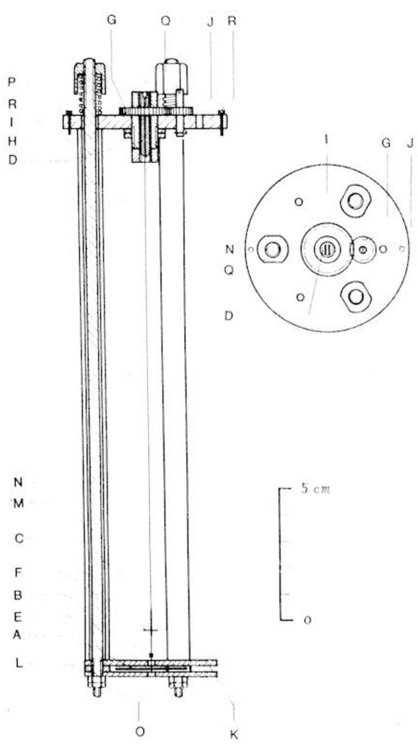

Figure 2. Suspension system. See Figure 1 for key.

transferred by using a Toepler pump (T). The quantity (moles) of the gas was determined from the volume, pressure, temperature of the system. The density of the gas was determined

Table II. Physical Properties of Components of Azeotropic Mixtures

	chem formula	mol wt[a]	T_b,[a] K	T_c,[a] K	P_c,[a] MPa	ρ_c,[a] kg·m^{-3}
R12	CCl_2F_2	120.914	243.5	384.95	4.125	558
R13	$CClF_3$	104.459	191.8	302.0	3.92	579
R22	$CHClF_2$	86.467	232.4	369.2	4.977	525
R23	CHF_3	70.014	191.1	298.8	4.84	526
R115	$CClF_2CF_3$	154.468	234.1	353.2	3.157	613
R152a	CH_3CHF_2	66.050	248.2	386.6	4.50	365

[a] Nomenclature and the data source are the same as in Table I.

Table III. Characteristics of the Suspension System at 298.15 K

distance between two fixed disks, mm	1.732
distance between the oscillating disk and the upper fixed disk, mm	0.388
distance between the oscillating disk and the lower fixed disk, mm	0.388
radius of the oscillating disk, mm	14.080
thickness of the oscillating disk, mm	0.959
moment of inertia of the suspension system, kg m^2	4.6057×10^{-7}
period of oscillation in vacuo, s	28.585
logarithmic decrement in vacuo	2.3×10^{-5}

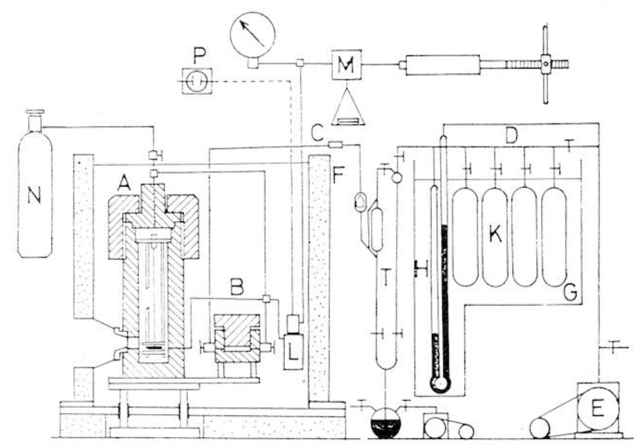

Figure 3. Schematic diagram of apparatus: A, viscometer; B, high-pressure pipet; C, connecting tube; D, connecting capillary; E, vacuum pump; F and G, thermostat; H, mercury manometer; K, glass cylinder; L, pressure difference detector; M, pressure balance; N, sample cylinder; P, pilot lamp; T, Toepler pump.

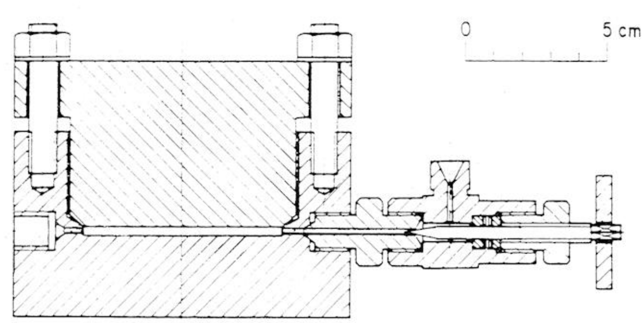

Figure 4. High-pressure pipet.

Table IV. Error Analysis in the Determination of the Gas Density

measured quantity		error, %
1. The Volume of the Expansion System (V_e)		
4 glass cylinders	1417.20 ± 0.08 cm^3	
connecting capillary	5.59 ± 0.02 cm^3	
mercury manometer	(0–50) ± 0.02 cm^3	
total (V_e)	1422.79 + (0–50) ± 0.12 cm^3	0.008
2. The Number of Moles of the Gas in the Expansion System (n)		
P = (750–770) ± 0.1 mmHg		0.013
V_e		0.008
z = (0.95–1) ± 0.0001		0.01
T = 298.15 ± 0.01 K		0.003
$n = PV_e/zRT$		0.034
3. The Volume of the High-Pressure Pipet (V_h)		
n		0.034
z for nitrogen (*17, 18*)		0.05
T = 298.15 ± 0.01 K		0.003
P = 12 ± 0.0001 MPa		0.001
$V_h = nzRT/P$ = 6.837 cm^3		0.088
4. The Gas Density (ρ)		
n		0.034
V_h		0.088
$\rho = n/V_h$		0.12

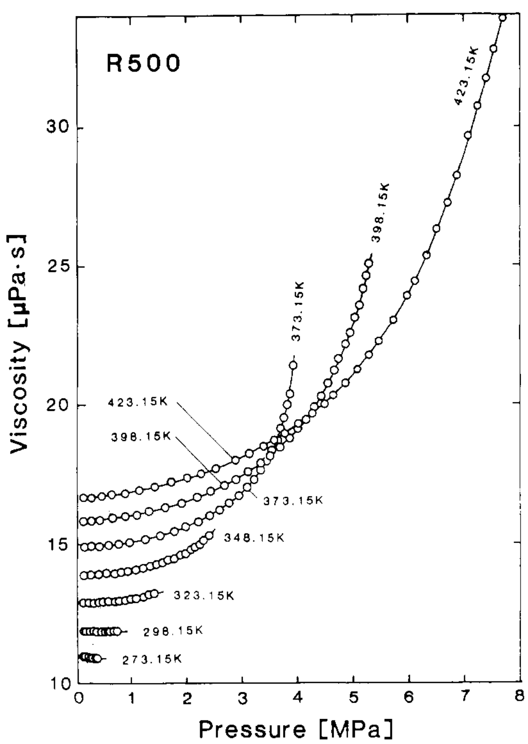

Figure 5. Gas viscosity vs pressure plots for R500.

from the above-determined gas quantity and the volume of the high-pressure pipet. The volume of the high-pressure pipet was determined as follows: the nitrogen (99.99% pure) was sampled into the pipet at 298.15 K and 12 MPa, and then introduced into the expansion system. The quantity of the nitrogen was determined by the procedure described above. Then, the volume of the pipet was calculated from the above determined gas quantity and the compressibility factor (*17, 18*). The volume of each part, the experimental condition, and the error analysis are shown in Table IV.

Substances. The azeotropic mixtures, the purities of which were certified to be 99.9%, were supplied by the Daikin Kogyo Co. and used without further purification. Gas chromatic analysis gave the same composition as shown in Table I and detected no impurities.

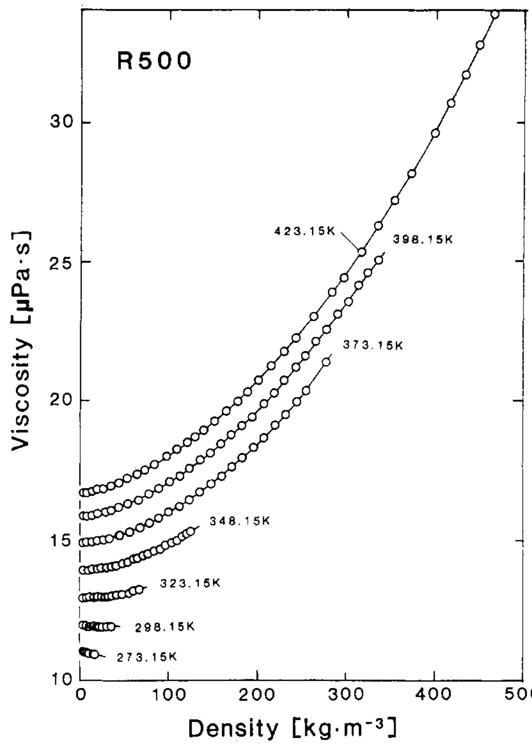

Figure 6. Gas viscosity vs density plots for R500.

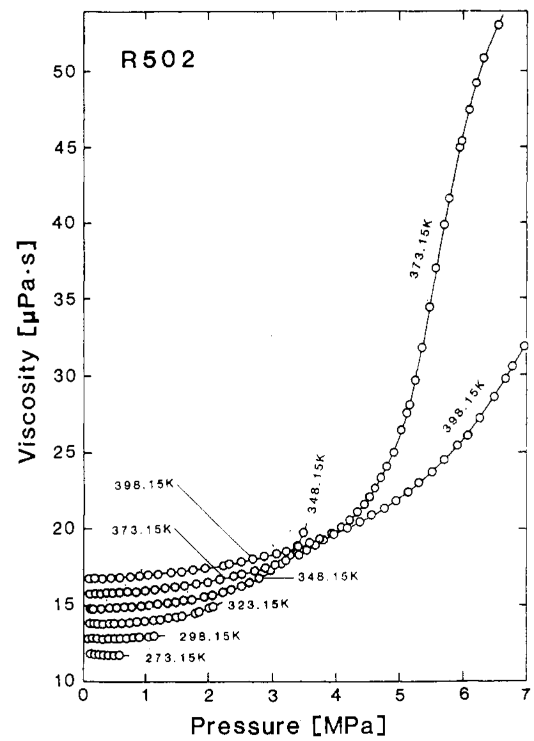

Figure 7. Gas viscosity vs pressure plots for R502.

Results and Discussion

The viscosity values obtained in the present measurement are shown in Tables V, VI, and VII and in Figures 5–10. Density values given in Table V and VII for R500 and R503 were obtained in this study, and those given in Table VI for

Table V. Gas Viscosity of R500

P, MPa	ρ, kg·m^{-3}	η, μPa·s	P, MPa	ρ, kg·m^{-3}	η, μPa·s	P, MPa	ρ, kg·m^{-3}	η, μPa·s	P, MPa	ρ, kg·m^{-3}	η, μPa·s
	273.15 K		0.5419	19.75	13.96	3.535	194.9	18.31	5.245	323.4	24.59
0.1052	4.603	11.00	0.6906	25.64	13.96	3.620	206.6	18.66	5.299	334.5	25.04
0.1499	6.819	10.98	0.8019	29.99	13.99	3.697	219.2	19.12			
0.1984	9.145	10.98	0.9359	35.68	14.03	3.762	230.7	19.51		423.15 K	
0.2475	11.58	10.95	1.070	41.49	14.08	3.817	242.7	19.96	0.1011	2.869	16.65
0.2975	14.13	10.94	1.203	48.07	14.13	3.863	253.8	20.35	0.1016	2.885	16.70
0.3512	16.98	10.94	1.336	53.96	14.21	3.893	265.8	20.86	0.2508	7.179	16.65
			1.451	59.86	14.28	3.926	276.8	21.38	0.4442	12.85	16.73
	298.15 K		1.562	65.72	14.32				0.6427	18.61	16.81
0.1017	4.154	11.94	1.658	71.60	14.41		398.15 K		0.8770	26.03	16.83
0.1531	6.312	11.92	1.774	77.67	14.47	0.1005	3.035	15.83	1.132	34.09	16.92
0.2051	8.547	11.91	1.879	84.04	14.59	0.2480	7.564	15.83	1.414	43.27	17.05
0.2647	11.17	11.91	1.975	90.43	14.65	0.3952	12.18	15.86	1.711	53.36	17.21
0.3283	14.09	11.90	2.073	97.09	14.80	0.6413	20.11	15.94	2.009	63.95	17.35
0.3982	17.29	11.89	2.147	103.2	14.89	0.8759	27.93	15.99	2.252	73.05	17.51
0.4754	21.02	11.90	2.229	109.1	14.97	1.090	35.46	16.06	2.530	83.83	17.70
0.5568	25.12	11.88	2.302	115.7	15.12	1.307	43.22	16.17	2.876	97.76	17.99
0.6441	29.72	11.89	2.373	121.6	15.22	1.597	53.93	16.31	3.131	108.7	18.24
0.7388	34.90	11.88	2.402	124.5	15.31	1.896	65.78	16.44	3.391	120.7	18.49
						2.169	77.26	16.66	3.577	129.3	18.69
	323.15 K			373.15 K		2.429	88.99	16.89	3.779	139.1	18.94
0.1020	3.829	12.92	0.1011	3.264	14.89	2.676	100.6	17.09	4.015	151.3	19.28
0.1029	3.838	12.92	0.1019	3.290	14.88	2.894	111.6	17.29	4.260	164.5	19.63
0.1917	7.296	12.92	0.2445	7.990	14.91	3.113	123.3	17.57	4.496	176.9	19.98
0.2838	10.96	12.91	0.3935	13.03	14.89	3.320	135.3	17.88	4.651	187.5	20.29
0.3934	15.47	12.92	0.5656	19.01	14.95	3.511	147.1	18.14	4.864	200.4	20.74
0.4971	19.81	12.95	0.7605	26.06	14.99	3.689	158.9	18.45	5.081	214.8	21.23
0.5868	23.71	12.95	0.9534	33.24	15.05	3.857	170.2	18.77	5.291	229.2	21.75
0.6820	28.04	12.96	1.243	44.94	15.16	4.013	182.1	19.11	5.465	242.7	22.24
0.7746	32.39	12.99	1.514	56.42	15.28	4.161	193.8	19.43	5.719	262.4	23.01
0.8876	37.74	13.00	1.764	67.59	15.44	4.298	205.8	19.89	5.965	283.1	23.87
0.9746	42.10	13.03	1.964	77.27	15.60	4.426	217.6	20.27	6.111	296.1	24.40
1.077	47.46	13.05	2.188	88.71	15.77	4.549	229.5	20.73	6.319	315.5	25.32
1.214	55.39	13.11	2.396	100.5	16.01	4.659	241.6	21.17	6.512	334.6	26.28
1.306	61.01	13.17	2.586	112.2	16.21	4.743	252.3	21.60	6.697	352.7	27.21
1.397	67.15	13.23	2.761	123.7	16.47	4.859	265.4	22.12	6.870	371.3	28.18
			2.927	135.7	16.72	4.953	277.5	22.54	7.074	396.7	29.62
	348.15 K		3.075	147.6	17.01	5.036	289.5	23.11	7.238	414.4	30.68
0.1015	3.518	13.91	3.209	159.4	17.28	5.116	301.0	23.55	7.391	431.3	31.69
0.1017	3.527	13.93	3.330	171.3	17.62	5.181	312.9	24.14	7.533	447.3	32.74
0.2479	8.730	13.90	3.439	183.0	17.95				7.688	463.5	33.83
0.3945	14.13	13.93									

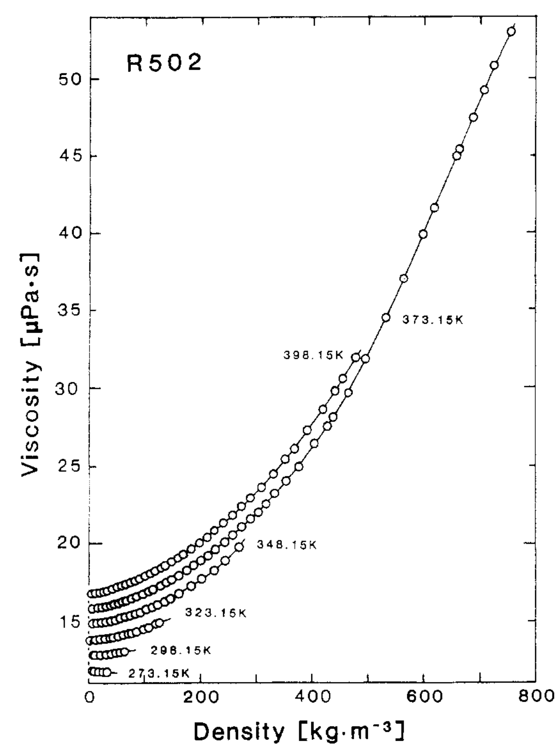

Figure 8. Gas viscosity vs density plots for R502.

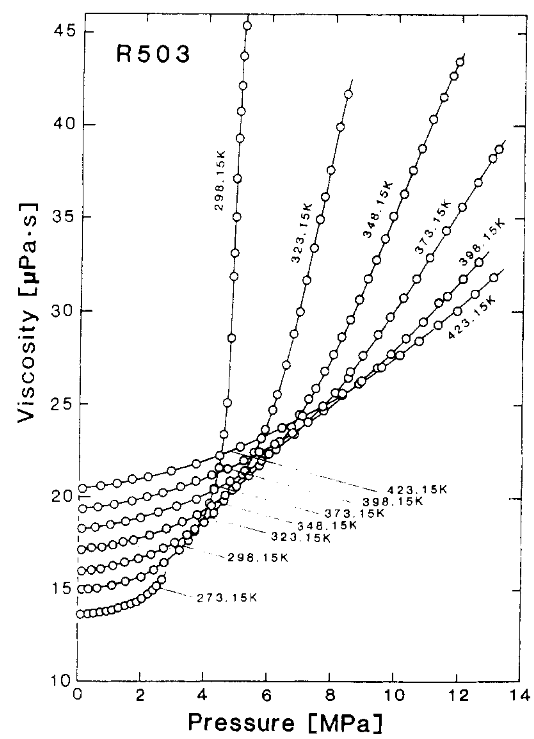

Figure 9. Gas viscosity vs pressure plots for R503.

R502 were calculated from the equation of state proposed by Martin et al. (*19*).

It will be noted that the viscosity vs pressure isotherms intersect as shown in Figures 5, 7, and 9, but the viscosity vs

Table VI. Gas Viscosity of R502

P, MPa	ρ, kg·m^{-3}	η, μPa·s	P, MPa	ρ, kg·m^{-3}	η, μPa·s	P, MPa	ρ, kg·m^{-3}	η, μPa·s	P, MPa	ρ, kg·m^{-3}	η, μPa·s
	273.15 K		1.850	105.5	14.59	0.9957	38.74	16.01		398.15 K	
0.1013	5.092	11.82	2.000	119.1	14.81	1.143	45.02	16.06	0.1013	3.440	16.75
0.1013	5.092	11.83	2.064	125.8	14.90	1.306	52.21	16.16	0.1672	5.695	16.76
0.1809	9.247	11.78				1.453	58.88	16.22	0.2158	7.373	16.79
0.2624	13.67	11.78		348.15 K		1.611	66.29	16.33	0.3101	10.65	16.78
0.3263	17.26	11.75	0.1013	3.945	14.82	1.804	75.67	16.44	0.4504	15.60	16.82
0.4013	21.64	11.75	0.1013	3.945	14.82	1.981	84.65	16.58	0.5983	20.92	16.84
0.4921	27.16	11.74	0.1773	6.955	14.83	2.163	94.26	16.73	0.7512	26.51	16.89
0.5604	31.59	11.74	0.2462	9.718	14.84	2.372	107.9	16.93	0.9043	32.23	16.93
			0.3344	13.31	14.84	2.514	114.2	17.07	1.052	37.87	17.03
	298.15 K		0.4124	16.54	14.87	2.706	127.9	17.30	1.202	43.68	17.07
0.1013	4.639	12.83	0.5259	21.34	14.88	2.872	136.6	17.49	1.407	51.87	17.17
0.1013	4.639	12.82	0.6434	26.43	14.91	3.028	147.2	17.72	1.577	58.82	17.25
0.1792	7.923	12.83	0.7784	32.44	14.94	3.195	159.2	17.98	1.746	65.93	17.35
0.2300	10.75	12.82	0.9216	39.02	14.98	3.388	174.2	18.34	1.935	74.10	17.45
0.3096	14.66	12.81	1.046	44.94	15.04	3.528	185.7	18.65	2.231	82.81	17.61
0.3952	19.00	12.83	1.181	51.56	15.11	3.662	197.5	18.94	2.320	91.49	17.74
0.4509	21.90	12.82	1.345	59.92	15.12	3.803	210.8	19.29	2.505	100.3	17.90
0.5077	24.92	12.82	1.473	66.76	15.26	3.931	223.8	19.68	2.677	109.6	18.07
0.5872	29.28	12.83	1.600	73.81	15.36	4.079	239.9	20.15	2.872	118.6	18.25
0.6951	35.44	12.86	1.726	81.08	15.42	4.203	254.8	20.62	3.060	128.5	18.45
0.7929	41.29	12.88	1.924	91.83	15.58	4.324	270.5	21.13	3.210	136.6	18.60
0.8993	48.01	12.90	2.055	101.6	15.73	4.434	286.0	21.63	3.406	147.7	18.85
1.041	57.63	12.94	2.212	112.5	15.89	4.524	300.0	22.10	3.590	158.5	19.10
1.128	63.95	12.99	2.345	122.3	16.06	4.612	314.7	22.65	3.744	167.9	19.34
			2.503	134.8	16.28	4.702	330.8	23.36	3.961	181.7	19.68
	323.15 K		2.626	145.4	16.49	4.800	350.4	24.13	4.181	196.5	20.09
0.1013	4.263	13.83	2.783	160.2	16.81	4.906	373.5	25.04	4.381	210.6	20.46
0.1013	4.263	13.84	2.976	180.9	17.30	5.024	402.4	26.51	4.563	224.1	20.90
0.1662	7.046	13.83	3.127	200.3	17.77	5.111	425.7	27.59	4.757	239.3	21.34
0.2305	9.849	13.82	3.268	221.6	18.34	5.146	435.6	28.16	4.952	255.4	21.84
0.3040	13.11	13.82	3.376	241.9	18.96	5.238	462.5	29.72	5.140	271.9	22.44
0.3962	17.29	13.83	3.481	267.3	19.80	5.344	494.1	31.84	5.313	287.8	23.04
0.5006	22.15	13.85				5.461	529.2	34.50	5.514	307.3	23.72
0.6156	27.68	13.87		373.15 K		5.551	561.2	37.04	5.713	329.6	24.54
0.7438	34.07	13.90	0.1013	3.674	15.80	5.699	596.4	39.93	5.922	350.2	25.48
0.8583	40.01	13.94	0.1013	3.674	15.80	5.774	616.1	41.64	6.070	367.0	26.21
0.9809	46.63	13.96	0.1824	6.653	15.81	5.943	656.3	45.00	6.266	390.0	27.29
1.118	54.37	14.04	0.2787	10.24	15.82	5.967	661.4	45.42	6.498	418.1	28.65
1.233	61.22	14.09	0.3668	16.57	15.84	6.085	685.5	47.49	6.672	439.7	29.82
1.360	69.23	14.18	0.4712	17.57	15.85	6.200	706.0	49.27	6.782	453.5	30.60
1.482	77.32	14.25	0.5816	21.87	15.88	6.313	723.9	50.91	6.966	476.6	31.94
1.576	83.99	14.32	0.7084	26.91	15.91	6.534	753.3	53.06			
1.723	97.07	14.46	0.8474	32.56	15.95						

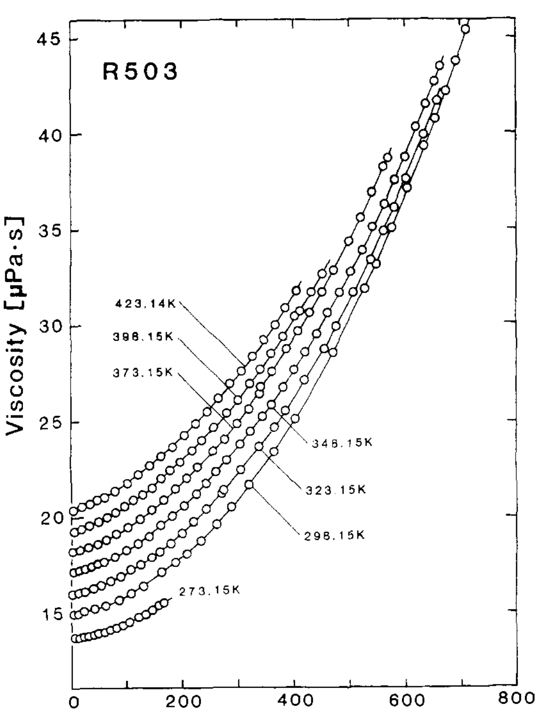

Figure 10. Gas viscosity vs density plots for R503.

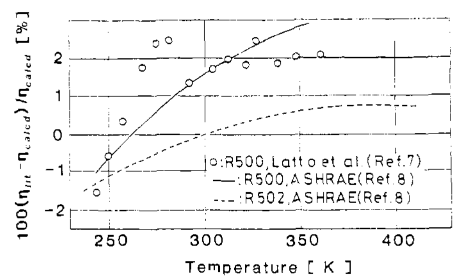

Figure 11. Deviations of the literature viscosity values from those calculated by eq 1 for R500 and R502.

density isotherms do not intersect, as shown in Figures 6, 8, and 10.

Equation 1 was obtained for the present experimental viscosity values at the atmospheric pressure as a function of temperature.

$$\eta_1 = a_1 T + a_2 T^2 \quad (1)$$

Constants in eq 1 and deviations of the experimental viscosity values from those calculated by eq 1 are shown in Table VIII. Table VIII shows that the reproducibility of eq 1 is satisfactory, because the maximum deviations (0.34% for R500 and 0.46% for R503) are not much larger than the estimated experimental error (0.3%).

Table VII. Gas Viscosity of R503

P, MPa	ρ, kg·m^{-3}	η, μPa·s
	273.15 K	
0.1020	3.961	13.68
0.1019	3.958	13.68
0.2939	11.65	13.69
0.4894	19.82	13.71
0.6863	28.45	13.79
0.8820	37.47	13.82
1.077	46.99	13.90
1.273	57.12	13.98
1.474	68.17	14.10
1.669	79.98	14.19
1.840	91.01	14.33
2.019	103.4	14.49
2.221	119.6	14.74
2.369	132.6	14.94
2.488	144.7	15.15
2.605	157.8	15.43
2.659	164.7	15.56
	298.15 K	
0.1022	3.628	14.94
0.1022	3.628	15.00
0.2977	10.74	15.01
0.6006	22.21	15.12
1.075	41.44	15.23
1.513	60.83	15.42
2.005	84.98	15.69
2.384	105.8	16.07
2.750	128.2	16.47
3.211	161.3	17.16
3.490	186.1	17.69
3.685	205.7	18.16
3.908	231.3	18.86
4.117	260.2	19.69
4.267	285.6	20.55
4.419	318.4	21.67
4.571	363.0	23.45
4.666	400.9	25.15
4.777	469.4	28.61
4.842	526.4	31.90
4.864	547.5	33.19
4.896	575.8	35.10
4.930	605.2	37.16
4.972	635.7	39.35
5.006	654.6	40.82
5.045	673.5	42.23
5.089	691.7	43.80
5.146	709.6	45.43
	323.15 K	
0.1018	3.330	16.03
0.1020	3.336	16.01
0.3934	13.11	16.07
0.7018	23.85	16.13
1.099	38.33	16.29
1.463	52.22	16.46
1.907	70.21	16.70
2.302	87.25	16.92
2.692	106.1	17.27
3.050	123.4	17.56
3.425	143.7	17.97
3.671	157.1	18.27
3.976	176.5	18.68
4.292	197.2	19.21
4.597	219.4	19.84
4.871	240.7	20.44
5.185	267.6	21.24
5.240	272.8	21.42
5.567	304.8	22.49
5.863	336.5	23.69
6.092	363.6	24.73
6.251	383.9	25.57
6.516	419.1	27.16
6.765	453.8	28.83
6.925	476.5	29.99
7.135	506.9	31.73
7.345	536.6	33.43
7.523	560.0	34.93
7.679	580.5	36.16
7.856	602.5	37.64
8.136	633.8	39.95
8.362	657.8	41.73
	348.15 K	
0.1018	3.088	17.18
0.1023	3.104	17.17
0.4002	12.34	17.28
0.7255	22.74	17.31
1.088	34.72	17.44
1.423	45.88	17.60
1.755	57.67	17.71
2.273	77.72	17.99
2.802	97.88	18.35
3.296	118.1	18.71
3.764	138.6	19.10
4.206	159.3	19.62
4.621	180.1	20.12
5.013	200.5	20.65
5.389	222.5	21.25
5.726	241.1	21.80
6.026	259.3	22.39
6.340	279.6	23.02
6.694	302.9	23.86
6.952	320.6	24.52
7.252	342.0	25.32
7.459	357.9	25.91
7.735	378.5	26.82
8.007	399.0	27.72
8.276	419.9	28.68
8.546	440.9	29.61
8.815	461.0	30.71
9.076	481.5	31.78
9.340	501.5	32.84
9.608	521.8	33.95
9.876	540.5	35.15
10.19	562.7	36.35
10.48	581.4	37.64
10.77	600.2	38.82
11.10	619.8	40.40
11.41	637.1	41.58
11.71	653.1	42.77
11.90	663.4	43.54
	373.15 K	
0.1017	2.875	18.42
0.1017	2.875	18.28
0.1024	2.896	18.32
0.4903	14.13	18.39
0.9714	28.55	18.52
1.496	44.83	18.70
1.963	59.61	18.90
2.518	78.02	19.20
3.101	98.68	19.55
3.721	121.2	19.96
4.267	141.9	20.45
4.790	163.2	20.95
5.298	184.6	21.51
5.777	205.5	22.06
6.232	226.1	22.66
6.806	253.3	23.47
7.240	274.7	24.13
7.657	295.4	24.92
8.069	316.5	25.69
8.461	337.1	26.48
8.523	338.1	26.83
8.919	359.1	27.68
9.410	385.7	28.82
9.797	406.3	29.76
10.19	427.7	30.76
10.59	448.9	31.81
11.01	469.9	32.94
11.50	497.7	34.43
11.99	518.5	35.66
12.49	540.1	36.98
12.96	560.8	38.30
13.16	569.3	38.78
	398.15 K	
0.1019	2.702	19.39
0.1022	2.707	19.38
0.5846	15.82	19.50
1.097	30.22	19.64
1.697	46.77	19.85
2.182	62.20	20.08
2.659	76.11	20.31
3.195	92.99	20.63
3.705	108.8	20.94
4.206	124.9	21.26
4.707	141.5	21.60
5.226	159.5	22.08
5.692	176.5	22.49
6.203	195.1	22.93
6.753	215.9	23.57
7.229	234.3	24.11
7.738	254.1	24.76
8.334	277.8	25.53
8.824	297.6	26.21
9.372	320.0	27.01
9.806	338.2	27.77
10.29	357.7	28.62
10.83	380.9	29.50
11.31	401.0	30.55
11.57	410.7	30.83
12.06	430.8	31.82
12.55	450.6	32.75
	423.15 K	
0.1010	2.519	20.47
0.1025	2.556	20.47
0.6877	17.57	20.62
1.208	31.35	20.77
1.678	43.62	20.97
2.191	57.71	21.13
2.905	77.21	21.45
3.705	99.85	21.84
4.411	120.3	22.28
5.092	140.8	22.77
5.751	161.1	23.24
6.409	181.8	23.77
7.045	202.4	24.37
7.679	223.3	24.99
8.290	243.8	25.60
8.903	264.2	26.30
9.504	285.0	27.03
10.09	305.3	27.71
10.69	325.4	28.47
11.28	345.6	29.32
11.89	366.5	30.10
12.44	384.9	30.98
13.04	404.6	31.87

Equation 2 was obtained for the present experimental viscosities in the whole range of pressure and temperature as a function of temperature and density. Constants in eq 2 are

$$\eta = b_0 + b_1\rho + b_2\rho^2 + b_3\rho^3 \quad (2)$$

$$b_0 = b_{01}T + b_{02}T^2 + b_{03}T^3 \quad (2.1)$$

$$b_1 = b_{10} + b_{11}T + b_{12}T^2 + b_{13}T^3 \quad (2.2)$$

$$b_2 = b_{20} + b_{21}T + b_{22}T^2 + b_{23}T^3 \quad (2.3)$$

$$b_3 = b_{30} + b_{31}T \quad (2.4)$$

given in Table IX, and deviations of the present experimental viscosity values from those calculated by eq 2 are shown in Table X and Figure 11. Table X shows that eq 2 is satisfactory for R500 and R502 from the same reason described about eq 1. The maximum deviations are larger for R503 at 298.15, 323.15, and 348.15 K. However, it should be noted that they occur in the highest density region (see Figures 9 and 10). Then, it can be said that eq 2 is satisfactory for R503 in the density range below 600 kg/m^3.

Table VIII. Constants in Eq 1 and Deviations of Experimental Viscosity Values at Atmospheric Pressure from Those Calculated by Eq 1

	R500	R502	R503
a_1	4.15976 × 10^{-2}	4.58808 × 10^{-2}	5.36971 × 10^{-2}
a_2	−4.87128 × 10^{-6}	−9.53395 × 10^{-6}	−1.24718 × 10^{-5}
T range, K	273.15–423.15	273.15–398.15	273.15–423.15
n[a]	7	6	7
dev,[b] %			
av	0.20	0.02	0.21
bias	−0.01	−0.00	−0.01
max	0.34	0.04	0.46

[a] n = number of data. [b] Deviation, av = $100\sum\{|\eta_{\text{exptl}} - \eta_{\text{calcd}}|/\eta_{\text{calcd}}\}/n$. Deviation, bias = $100\sum\{(\eta_{\text{exptl}} - \eta_{\text{calcd}})/\eta_{\text{calcd}}\}/n$. Deviation, max = maximum of $100|\eta_{\text{exptl}} - \eta_{\text{calcd}}|/\eta_{\text{calcd}}$.

The density of R500 can be calculated by eq 3 (*20*), the constants of which were determined by the present authors using the present experimental density values and are shown in Table XI. Deviations of the present experimental density

Table IX. Constants in Eq 2

	R500	R502	R503
b_{01}	4.21248×10^{-2}	4.65472×10^{-2}	5.44946×10^{-2}
b_{02}	-6.46990×10^{-6}	-1.16797×10^{-5}	-1.48308×10^{-5}
b_{10}	-1.15943×10^{-1}	-8.90508×10^{-2}	-2.77843×10^{-2}
b_{11}	5.66237×10^{-4}	4.46167×10^{-4}	1.40920×10^{-4}
b_{12}	-6.5209×10^{-7}	-5.16951×10^{-7}	-1.17507×10^{-7}
b_{20}	7.19×10^{-5}	3.49920×10^{-4}	8.00691×10^{-5}
b_{21}	0	-1.61430×10^{-6}	-8.75862×10^{-8}
b_{22}	0	2.20661×10^{-9}	0
b_{30}	1.525×10^{-8}	0	0
b_{31}	-7.6×10^{-11}	0	0

Table X. Deviations of Experimental Viscosity Values from Eq 2

temp, K	P range, MPa	ρ range, kg·m^{-3}	n[a]	dev,[b] %		
				av	bias	max
		R500				
273.15	0.3512	16.98	6	0.34	+0.34	0.59
298.15	0.7388	34.90	10	0.19	−0.19	0.30
323.15	1.397	67.15	15	0.11	+0.01	0.32
348.15	2.402	124.5	23	0.14	+0.08	0.44
373.15	3.926	276.8	28	0.13	+0.01	0.38
398.15	5.299	334.5	32	0.28	−0.13	0.95
423.15	7.688	463.5	37	0.29	−0.22	0.71
		R502				
273.15	0.560	31.46	8	0.07	−0.01	0.14
298.15	1.128	63.96	14	0.06	−0.01	0.11
323.15	2.064	126.7	20	0.12	−0.11	0.31
348.15	3.481	273.0	28	0.13	−0.06	0.55
373.15	5.344	492.6	42[c]	0.15	+0.06	0.36
398.15	6.266	382.1	37[d]	0.17	−0.08	0.91
		R503				
273.15	2.659	164.7	17	0.65	−0.65	0.94
298.15	5.146	709.6	28	0.55	+0.55	1.42
323.15	8.362	657.8	32	0.60	−0.45	1.46
348.15	11.90	663.4	38	0.43	−0.32	1.32
373.15	13.16	572.8	32	0.26	+0.18	0.78
398.15	12.55	450.6	27	0.15	−0.08	0.43
423.15	13.04	404.6	23	0.13	+0.01	0.33

[a] n = number of data. [b] Definition of deviations is the same as in Table VIII. [c] 10 data were omitted from 5.461 to 6.534 MPa. [d] Four data were omitted at pressures from 6.498 to 6.966 MPa.

Table XI. Constants in Eq 3, Equation of State for R500

$R = 0.0820568$ L·atm·K^{-1}·mol^{-1}	$a = 0.18949366 \times 10$
$A_0 = 2.2454666$	$b = 0.40383132 \times 10^{-1}$
$B_0 = 0.80445386 \times 10^{-2}$	$c = 0.15868914 \times 10^{6}$
$C_0 = 0.89637405 \times 10^{6}$	$e = -0.64800314 \times 10^{2}$
$D_0 = 0.27927010 \times 10^{8}$	$e = -0.50668022 \times 10^{9}$
$E_0 = -0.12047885 \times 10^{10}$	$f = -0.19238439 \times 10^{39}$
	$g = 0.30061305 \times 10^{15}$
	$h = -0.28904021 \times 10^{32}$
	$\alpha = 0.38452516 \times 10^{-3}$
	$\gamma = 0.20299265 \times 10^{-1}$

values from those calculated by eq 3 are shown in Table XII. They are of the same order in the temperature range from 273.15 to 373.15 K as those from the equation of state proposed by Sinka et al. (*21*), and smaller at 398.15 and 423.15 K.

$$P = RT\rho + (B_0RT - A_0 - C_0/T^2 + D_0/T^3 - E_0/T^4)\rho^2 + (bRT - a - d/T - e/T^4 - f/T^{23})\rho^3 + \alpha(a + d/T + e/T^4 + f/T^{23})\rho^6 + (c/T^2 + g/T^8 + h/T^{17})\rho^3(1 + \gamma\rho^2)\exp(-\gamma\rho^2) \quad (3)$$

The density of R503 can be calculated by the equation of state proposed by Sinka et al. (*22*). Deviations of the experimental density values from those calculated by this equation are shown in Table XIII. Reasonable constants of eq 3 could not be obtained for R503.

Table XII. Deviations of Present Experimental Density Values of R500 from Those Calculated by Eq 3

temp, K	P range, MPa	ρ range, kg·m^{-3}	n[a]	dev,[b] %		
				av	bias	max
273.15	0.3512	16.98	6	0.07	−0.07	0.11
298.15	0.7388	34.90	10	0.09	+0.04	0.39
323.15	1.397	67.15	15	0.38	−0.21	0.95
348.15	2.402	124.5	23	0.45	−0.44	0.93
373.15	3.926	276.8	28	0.96	+0.94	5.42
373.15[c]	3.620	206.6	22	0.33	+0.30	1.30
398.15	5.299	334.5	32	0.55	+0.52	1.67
423.15	7.688	463.5	37	0.49	+0.40	1.29

[a] n = number of data. [b] Deviation, av = $100\sum\{|\rho_{\rm exptl} - \rho_{\rm calcd}|/\rho_{\rm calcd}\}/n$. Deviation, bias = $100\sum\{(\rho_{\rm exptl} - \rho_{\rm calcd})/\rho_{\rm calcd}\}/n$. Deviation, max = maximum of $100|\rho_{\rm exptl} - \rho_{\rm calcd}|/\rho_{\rm calcd}$. [c] Six data at pressures above 3.697 MPa were omitted.

Table XIII. Deviations of the Present Experimental Density Values of R503 from Those Calculated by the Equation of State Proposed by Sinka et al. (*22*)

temp, K	P range, MPa	ρ range, kg·m^{-3}	n[a]	dev,[b] %		
				av	bias	max
273.15	2.654	164.7	17	1.76	−1.76	2.54
298.15	5.146	709.6	28	1.45	−1.45	2.69
323.15	8.362	657.8	32	1.15	−1.14	1.54
348.15	11.90	663.4	38	0.94	−0.93	1.61
373.15	13.16	569.3	32	1.08	−1.08	2.78
398.15	12.55	450.6	27	1.13	−1.09	1.77
423.15	13.04	404.6	23	0.95	−0.77	1.58

[a] n = number of data. [b] Definition of deviation is the same as in Table XII.

Glossary

A_0–E_0	constants in eq 3
P	pressure, MPa or atm
R	gas constant (=0.0820568 L·atm·K^{-1}·mol^{-1})
T	temperature, K
a	constant in eq 3
a_i	constants in eq 1 (i = 1, 2)
b	constant in eq 3
b_i	constants in eq 2 (i = 0, 1, 2, 3)
b_{0i}	constants in eq 2.1 (i = 1, 2, 3)
b_{1i}	constants in eq 2.2 (i = 0, 1, 2, 3)
b_{2i}	constants in eq 2.3 (i = 0, 1, 2, 3)
b_{3i}	constants in eq 2.4 (i = 0, 1)
c–h	constants in eq 3
α, γ	constants in eq 3
η	viscosity, μPa·s
η_1	viscosity at atmospheric pressure, μPa·s
ρ	density, kg·m^{-3} or mol·L^{-1}

Registry No. R500, 56275-41-3; R502, 39432-81-0; R503, 50815-73-1.

Literature Cited

(1) Takahashi, M.; Takahashi, S.; Iwasaki, H. *Kagaku Kogaku Ronbunshu* **1983**, *9*, 482.
(2) Takahashi, M.; Takahashi, S.; Iwasaki, H. *Kagaku Kogaku Ronbunshu* **1984**, *10*, 7.
(3) Takahashi, M.; Takahashi, S.; Iwasaki, H. *J. Chem. Eng. Data* **1985**, *30*, 10.
(4) Takahashi, M.; Yokoyama, C.; Takahashi, S. *Kagaku Kogaku Ronbunshu* **1985**, *11*, 155.
(5) Takahashi, M.; Yokoyama, C.; Takahashi, S. *J. Chem. Eng. Data* **1987**, *32*, 98.
(6) Makita, T. *Viscosity and Thermal Conductivity*; Baifukan: Tokyo, 1975; p 224–226.
(7) Latto, B.; Hesoun, P.; Asrani, S. C. *Proc. 5th ASME Symp. Thermophys. Prop.* **1970**, 177.
(8) *Thermophysical Properties of Refrigerants*; American Society of Heating, Refrigerating and Air-Conditioning Engineers Inc.: New York, 1976.
(9) *Transport Properties of Freon Fluorocarbons*; Tech. Note C30; Du Pont de Nemours and Co., Inc., 1967.
(10) Iwasaki, H.; Takahashi, H. *Bull. Chem. Res. Inst. Non-Aqueous Solutions, Tohoku University* **1956**, *6*, 61.
(11) Iwasaki, H.; Takahashi, M. *Rev. Phys. Chem. Jpn.* **1968**, *38*, 18.

(12) Newell, G. F. *Z. Angew. Math. Phys.* **1959**, *10*, 160.
(13) Iwasai, H.; Kestin, J. *Physica* **1963**, *29*, 1345.
(14) Hanley, H. J. M.; Ely, J. F. *J. Phys. Chem. Ref. Data* **1973**, *2*, 735.
(15) Hanley, H. J. M.; McCarty, R. D.; Haynes, W. M. *J. Phys. Chem. Ref. Data* **1973**, *2*, 735.
(16) Iwasaki, H.; Takahashi, M. *Proc. 4th Conf. High Pressure, Kyoto 1974*; Physicochemical Society of Japan: Kyoto, 1974; p 523.
(17) Michels, A.; Lunbeck, R. J.; Wolkers, G. J. *Physica* **1951**, *17*, 801.
(18) Michels, A.; Gibson, R. O. *Ann. Phys.* **1928**, *87*, 850.
(19) Martin, J. J.; Downing, R. C. *ASHRAE Trans. Part II* **1970**, 129.
(20) Nishiumi, H.; Saito, S. *J. Chem. Eng. Jpn.* **1965**, *8*, 356.
(21) Sinka, V. J.; Murphy, K. P. *J. Chem. Eng. Data* **1967**, *12*, 315.
(22) Sinka, J. V.; Rosenthal, E.; Dixon, P. P. *J. Chem. Eng. Data* **1970**, *15*, 73.

Received for review April 7, 1987. Revised February 9, 1988. Accepted March 9, 1988. We thank the Daikin Kogyo Co. for supplying the samples.

Vapor–Liquid Equilibria in the Methane–Diethylene Glycol–Water System at 298.15 and 323.15 K

Chiaki Yokoyama,* Shigeru Wakana, Gen-ichi Kaminishi, and Shinji Takahashi
Chemical Research Institute of Non-Aqueous Solutions, Tohoku University, Sendai 980, Japan

The water contents of compressed methane gas in equilibrium with water and diethylene glycol–water solutions of 0.156, 0.472, and 0.662 mole fraction water were measured at 298.15 and 323.15 K and pressures of 3, 5, and 8 MPa. The solubilities of methane in the diethylene glycol, water, and diethylene glycol–water solutions were also measured under the same conditions of the water content measurement. The methane solubility data were analyzed with the Krichevsky–Kasarnovsky equation to obtain the Henry constant of methane in the diethylene glycol–water solutions.

Gas dehydration plays an important part in gas purification processes. Diethylene glycol and triethylene glycol are effective gas dehydrating agents. A knowledge of the vapor–liquid equilibria in the gas–glycol–water system is helpful in designing an effective dehydration system. Takahashi et al. (*1*) have reported the vapor–liquid equilibrium data in the carbon dioxide–diethylene glycol–water and carbon dioxide–triethylene glycol–water systems. In this study, we measured the vapor–liquid equilibria in the methane–diethylene glycol–water system at 298.15 and 323.15 K and pressures of 3, 5, and 8 MPa.

Among the binary systems made up of methane, diethylene glycol, and water, the vapor–liquid equilibrium data for the methane–water system have been studied extensively. The solubility of methane in water was measured by Michels et al. (*2*) at temperatures from 298.15 to 423.15 K and at pressures up to 20 MPa, by Culberson and McKetta (*3*) at temperatures from 298 to 444 K and at pressures up to 69 MPa, and by O'Sullivan and Smith (*4*) at temperatures from 323 to 398 K and at pressures up to 61 MPa. The water content in methane was measured by Olds et al. (*5*) at temperatures from 310.7 to 510.8 K and at pressures up to 69 MPa, and by Rigby and Prausnitz (*6*) at temperatures from 298.15 to 373.15 K and at pressures up to 9.3 MPa. The vapor–liquid equilibria in the methane–water system were measured by Gillespie and Wilson (*7*) at temperatures from 323.15 to 588.71 K and at pressures up to 14 MPa. The vapor–liquid equilibria in the diethylene glycol–water system was measured by Jelinek et al. (*8*). Russell et al. (*9*) measured the vapor–liquid equilibria in the natural gas (94% methane)–aqueous diethylene glycol (5 wt % water) system at a temperature of 310.93 K and at pressures up to 13.8 MPa.

Experimental Procedure

The measurements of this study were made in a vapor recirculating static apparatus. The schematic diagram is shown in Figure 1. The equilibrium cell is a 100 cm^3 dual window model constructed by Ruska Instrument Corp. Samples were withdrawn from the equilibrated phases through $^1/_{16}$-in. 316 stainless steel tubing. The bath temperature was controlled to within ±0.02 K with a thermistor controller and measured by the mercury thermometer, which was calibrated by a Leeds-Northrup platinum resistance thermometer with an accuracy 0.01 K. The pressure of the cell was measured with a strain gauge pressure transducer calibrated periodically by a dead weight pressure gauge. The accuracy of the pressure measurement was estimated to be 1 kPa. To promote attainment of equilibrium, the vapor phase was circulated by means of a magnetic recirculation pump. The function of the pump was to withdraw the vapor from the top of the cell and discharge the vapor into the bottom of the cell. After the vapor was recirculated about 2 h, the vapor and liquid phases were allowed to remain stationary to ensure a complete separation of the phases.

The diethylene glycol–water solutions used for the ternary system were prepared by adding water to diethylene glycol until the binary mixture reached a predetermined weight. Weighings were performed on a Sartorius analytical balance capable of precision to at least 0.1 mg. The accuracy of the determination of the composition was within a mole fraction of 0.0002. After the cell was evacuated by a vacuum pump, the solution was fed to the cell. Then methane was bubbled into the solution for 30 min to saturate the solution with methane and discharge other light gases dissolved in the solution. After the degassing procedure, the final composition of the solution was checked by a Karl-Fisher titration apparatus but was found not to change appreciably.

Methane was then added to the cell to adjust the cell pressure. The bath was heated to the desired temperature and the vapor was recirculated by the magnetic pump. Samples of each phases were withdrawn from the cell through $^1/_{16}$-in. tubings, which were heated to prevent a condensation of water and diethylene glycol. After the contents in the sampling line was purged out about 1 cm^3, a sample of 3–5 cm^3 was withdrawn into a sample train and weighed with an accuracy of 0.1 mg.

Sample Analysis

The methane dissolved in the liquid-phase sample was collected in a gas buret with the use of a Toepler pump. The volume of the gas buret was calibrated with mercury to within ±0.01 cm^3. The details of the gas buret and Toepler pump were described by Arai et al. (*10*). The quantity of methane was determined from the pressure, volume, and temperature in the expanded state. The pressure after expansion was

